# Chapter I

## Population sparsening and temporal sharpening of olfactory representations in the honeybee mushroom bodies


## Summary

We characterized odor-evoked network activity in an insect brain at three consecutive neural compartments. Using $Ca^{2+}$ imaging, we recorded activity in the dendrites of the projection neurons that connect the antennal lobe with the mushroom body, a higher-order integration center. Next, we recorded the presynaptic terminals of these projection neurons. Finally, we characterized their postsynaptic partners, the intrinsic neurons of the mushroom body, the clawed Kenyon cells. Odors evoked combinatorial activity patterns at all three processing stages, but the spatial patterns became progressively sparsened along this path. Furthermore, Kenyon cells integrated projection neuron activities within 200 ms and transformed complex temporal patterns into brief phasic responses. Thus, two types of transformations occurred: Sparsening of the combinatorial code, depending on pre- and postsynaptic processing within the MB microcircuits, and temporal sharpening of postsynaptic Kenyon cell responses, probably involving a broader loop of inhibitory recurrent neurons.


## Introduction

The main olfactory brain regions in insects are the antennal lobes (AL) and the mushroom bodies (MB) (Figure 1.1A). The AL is the first synaptic processing station and a functional homologue to the vertebrate olfactory bulb (Hildebrand and Shepherd, 1997). The AL of honeybees consists of about 160 sub-compartments, called glomeruli (Flanagan and Mercer, 1989; Galizia et al., 1999a). In many species receptor neurons expressing the same receptor gene converge onto a single glomerulus (Mombaerts et al., 1996; Vosshall et al., 2000), and functional data

suggest that this holds true in the bee (Galizia et al., 1999b). PNs convey the output of glomeruli to higher brain areas via different axonal tracts (Mobbs, 1982; Bicker et al., 1993). Two of these tracts, the median and the lateral antenno-cerebralis tracts (m- and l- ACT) are composed of uniglomerular PNs and target the lateral horn and the MB (Abel et al., 2001; Müller et al., 2002). The MBs are higher-order integration centers that play a dominant role in odor learning (Davis, 1993; Menzel, 1999; Heisenberg, 2003). They are densely packed with 170,000 Kenyon cells (KC). KC dendrites receive second-order sensory input in the MB calyces, with different modalities innervating spatially distinct areas (Mobbs, 1982; Gronenberg, 1986; Schröter and Menzel, 2003). Olfactory input is confined to the lip region. KC axons target output neurons in the α- and β-lobes of the MB (Kenyon, 1896; Mobbs, 1982; Rybak and Menzel, 1993). In these areas, GABAergic feedback neurons receive input and project back to the MB lip region, forming a global inhibitory loop (Schäfer and Bicker, 1986; Grünewald, 1999a). Electrophysiological recordings in locusts and imaging experiments in *Drosophila* indicate that odor representations do indeed differ remarkably in the AL and the MB. Unlike PNs, KCs respond to odors in a sparse way: KCs appear to be much more odor-specific than PNs and generate fewer action potentials in response to odors (Perez-Orive et al., 2002; Stopfer et al., 2003; Wang et al., 2004). However, it is unclear whether this transformation of odor representation is a result of general feed-forward inhibition (as suggested for locust), or pre- and/or postsynaptic processing within the MB lip region. In the MB lip, the bouton-like PN terminals are involved in reciprocal microcircuits between GABAergic neurons and PNs (Figure 1.1C) (Ganeshina and Menzel, 2001). The existence of these circuits indicates that the information-flow from PNs onto KCs may not only be shaped by feed-forward processes, but may include interactions between PNs and GABAergic neurons within the MB microcircuits. We have therefore addressed the question of whether output activity of PN boutons is modified by presynaptic processing within the MB.

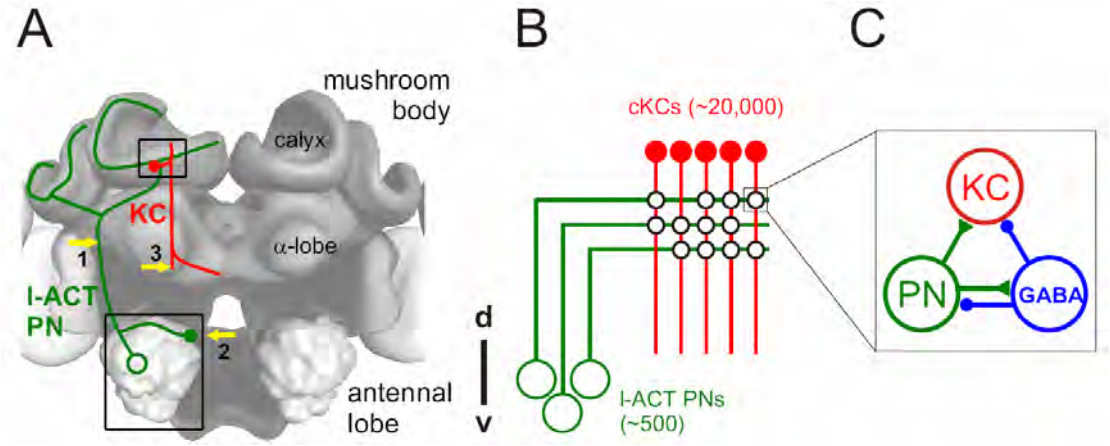


**Figure 1.1 The olfactory pathway in the bee brain**

**(A)** Scheme of the bee brain. l-ACT projection neurons (PN, green) were optically recorded at their dendrites in the antennal lobe (AL) and at their presynaptic boutons in the lip of the mushroom body (MB) calyx. Dendrites and somata of clawed Kenyon cells (cKC, red) were recorded in the MB calyx. Yellow arrows indicate sites of dye injection: 1 for recording PN dendrites in the AL, 2 for recording PN boutons in the MB calyces, and 3 for recording KCs in the MB calyces. Squares represent the two imaged areas, AL (for measuring PN dendrites) and MB calyx (for measuring PN boutons and/or cKCs). **(B)** The wiring diagram illustrates the divergent-convergent connectivity between PNs and cKCs. About 400 cholinergic l-ACT PNs synapse onto roughly 20,000 cKCs. The dendrites of cKCs are small, arranged in columns, and feature few claw-like synaptic specializations (black circles). **(C)** Within the lip region, PNs synapse onto GABAergic neurons which, in turn, make inhibitory synapses with PNs and KCs (adapted from Ganeshina and Menzel, 2001, with permission). Moreover, GABAergic feedback neurons receive input in the MB lobes and send their axons to calyx lip region. Since they leave out the ventral alpha lobe, they presumably do not receive input from cKCs. Thus, GABAergic neurons may provide local, PN-driven inhibitory microcircuits within the MB calyx lip, and a more global inhibitory feedback loop between the MB output and input region.

KCs of the lip region can be classified into two different groups based on their anatomy (Mobbs, 1982; Rybak and Menzel, 1993; Strausfeld, 2002; Farris et al., 2004): Class I KCs with somata located inside the calyx, and clawed KCs (also called class II or type 5 KCs) with somata outside the calyx. The term “clawed” refers to characteristic claw-like postsynaptic specializations at their dendrites. Honeybee clawed KCs (cKC) are likely to be homologues to *Drosophila* clawed KCs whose axons constitute the MB γ-lobe (Strausfeld, 2002). These cells are crucial for short term olfactory memory in *Drosophila* (Zars et al., 2000). Therefore, the bees’ cKCs may also play an important role in odor learning.

Until now, nothing was known about the physiological properties of these KCs and about their role in olfactory coding. In this study we therefore recorded odor-evoked responses in cKCs and compared them to their presynaptic input from l-ACT PNs, both in their boutons at the cKC synapse, and in their dendrites within the AL glomeruli. At all three processing stages, odors reliably evoke combinatorial activity patterns. However, in contrast to PNs, cKCs code odors in a sparse way, and generate only brief responses at stimulus onset. We found that the high odor-specificity of the cKCs originates at two steps, first, in a presynaptic sharpening of projection neuron synaptic output, and second, in a reduction in cKC response. Interestingly, the temporal sharpening of cKCs' responses is established only at the postsynaptic side. Our results also indicate that PN spikes generated within the first 200 ms determine whether a cKC will respond, while later PN spikes do not contribute to their activity.

# Material and Methods

### *In vivo* bee preparation and dye loading

Experiments were performed with forager bees, *Apis mellifera carnica*. Bees were collected at the hives, chilled and fixed as a whole animal into recording chambers. In order to prevent visual stimulation through light exposure during optical recordings the complex eyes were covered with dental wax mixed with charcoal. To allow access to the brain, the head capsule was opened by removing a piece of cuticle surrounded by the antennae, the ocelli and the complex eyes. Where necessary, pieces of trachea covering the injection sites were removed. Neurons were stained with dextran-conjugated $Ca^{2+}$ indicators by mass-injection (Fura-2 dextran, Calcium Green-1 dextran, Molecular Probes, Eugene). Injection needles were pulled from 1 mm glass capillaries to a tip diameter of ~10 µm and were coated with dye dissolved in 2% solution of bovine serum albumin. PN dendrites in the AL were retrogradely stained with Fura-2 dextran *via* their axons running through the l-ACT, PN axon terminals were anterogradely stained with either Fura-2 dextran or Calcium Green-1 dextran *via* l-ACT PN soma clusters in the dorso-medial part of the ALs, and dendrites and somata of cKCs were retrogradely stained by injecting Fura-2 dextran into the cKC axons located in the ventral part of the α-lobes (see Figure 1.1). Application of $Ca^{2+}$

indicators with different fluorescence spectra for cKC and PN bouton staining allowed simultaneous recording of cKCs and PN boutons. After dye injection the head capsule was closed with the cuticle piece and sealed with *n*-eicosan (Sigma). Half an hour later, bees were fed until satiation and kept in a container at 17°C to 20°C for 8 to 24 hours. To prevent movement artifacts, abdomen and legs were immobilized with dental wax, muscles which innervate the antennae were carefully removed, the mouthparts were truncated and the esophagus was taken out. Immediately afterwards, the head capsule was washed with bee Ringer (in mM: 130 NaCL, 7 $CaCl_2$, 6 KCl, 2 $MgCl_2$, 160 sucrose, 25 glucose, 10 HEPES, pH 6.7, 500 mOsmol). In order to stabilize the brain, a 1.5 % solution of low-melting agarose (Sigma, A2576) was injected into the head capsule. Experiments started 30 min after preparation.

**Odor stimulation and imaging**

We used the following odors: 1-hexanol, 2-octanol, limonene, linalool (all from Sigma) and peppermint oil (local drugstore). Odors were diluted in mineral oil in order to reduce evaporation and to adjust for differences in vapor pressure. Concentrations were as follows: 1-hexanol 16.2 %, 2-octanol, 60 %, limonene 9 % and linalool 46.2 %. 4 µl of the odor solution were applied onto a 2 $cm^2$ piece of filter paper and placed in a plastic syringe. Using a computer controlled olfactometer (Galizia et al., 1997), odors were injected into a continuous air stream which was directed to both antennae. Odors were presented as 3-second pulses 3 or 6 times in a pseudo-randomized order with a 1-minute inter-stimulus interval.

Images were acquired at room temperature with a sampling rate of 5 Hz using a TILL-Photonics imaging set up mounted on a fluorescence microscope (Olympus BX-50WI). Measurements started 2 seconds before stimulus onset and lasted for 12 s. In the AL, l-ACT PN dendrites were recorded through an 20x, 0.95 W Olympus objective. Fura-2 was excited at a single wavelength (390 nm) in order to reduce photodamage. Fluorescence was detected through a 410 nm dichroic mirror and a 440 nm long pass filter with an Imago-QE CCD camera (1376 x 1040 pixel, 8x binned on chip to 172x130). In the median MB calyx, KCs and PN boutons were recorded through a 60x, 0.9 W Olympus objective with an Imago CCD camera (640 x 480 pixel, 4x binned on chip to 160x120). The spatial resolution was 1.3 µm² per pixel

and allowed resolving single l-ACT PN boutons and cKC dendrites and somata. Fura-2 measurements of cKCs and PN boutons were carried out with the same filter settings used for l-ACT PN dendrite recordings. For simultaneous recording of cKCs (Fura-2) and l-ACT PN boutons (Calcium Green-1) the MB calyx was illuminated alternately with 390 nm and 475 nm at rate of 10 Hz; the fluorescence was detected through a Omega 505DRLPXR dichroic mirror and a 515 nm LP filter.

**Data analysis**

Data were analyzed using custom-written programs in IDL (RSI, Boulder, Colo., USA). For morphological images raw fluorescence images were unsharp mask filtered in Photoshop (Adobe, USA). $Ca^{2+}$ signals were calculated as fluorescence change relative to background fluorescence ($\Delta F/F$). Background fluorescence (F) was determined by an average of 5 frames obtained before stimulation and was subtracted from every frame of a measurement to give $\Delta F$. Signals were corrected for dye bleaching by subtracting a logarithmic curve fitted to the mean brightness decay of the entire image frames, excluding frames during the stimulus. Since the same value was subtracted from each pixel within a frame, the bleach correction did not affect the spatial activity pattern of the $Ca^{2+}$ signals (Galizia and Vetter, 2004). Signals of Fura-2 have been inverted, since it decreases its fluorescence at 390 nm excitation light in response to increasing $Ca^{2+}$ concentrations. Activity patterns are depicted as color-coded images, representing the averaged $\Delta F/F$ values of 15 frames (3 s) during the odor stimulus. For better visualization a spatial low-pass filter (3 x 3 pixels) was applied onto the images. To analyze the response dynamics, activity patches, corresponding to responsive PN dendrites, PN boutons, KC dendrites and KC somata during the 3-second odor-pulse, were selected. These pixels were averaged without filtering. The time courses obtained were then analyzed in Excel (Microsoft, USA). For analyzing the dynamics of $Ca^{2+}$ signals 3 measurements were averaged. Noise was defined pixel wise as the standard deviation of the fluorescence values over a 2-second interval (10 frames) before odor stimulus. To determine the proportion of excitatory and inhibitory responses only signals with amplitudes above 5 times noise were analyzed. To determine the onset of responses only signals 7 times above noise were analyzed. The response onset was defined as signal above 3 times noise.

Correlation analysis of spatial activity patterns was performed by computing the linear correlation between them. In order to determine the response profiles of PN dendrites, boutons and KC somata, three measurements were averaged. Since KCs respond within 600 ms after the stimulus onset (Figure 1.6B), only responses occurring within the first three frames (600 ms) after stimulus onset were considered for PNs and KCs, in order to achieve comparability. Signals were considered as responses if the averaged signal during the first three frames was 3 times greater than noise. Isolated activity spots smaller than 2 x 2 pixels (2.6 $\mu m^2$) were regarded as noise and rejected. In order to detect responses of individual KC somata or PN boutons, scattered light was reduced by applying an unsharp mask filter (Galizia and Vetter, 2004). For unsharp mask-filtering images were low-pass filtered (30 µm kernel size) and subtracted from two times the original signals. Thus images were sharpened while the absolute signal strength remained unchanged.

Due to variability in dye loading, the number and identities of stained PN boutons and KCs differed between preparations. Therefore we pooled the data coming from different animals for analyzing response profiles shown in Figures 1.3 and 1.5. Since the probability of recording the same boutons or KCs in two different preparations was very low, we assume that pooled data reveal general properties of the l-ACT PN boutons and cKCs. Although the number and identity of the PNs recorded in the AL glomeruli were similar between animals, and in order to make the AL data comparable to the MB data, the former were also pooled. Furthermore, within-animal analysis was performed for the AL data showing no differences to the pooled analysis (data not shown).

For evaluating how many PN boutons have to be activated for one KC to fire we used binominal distribution (which in case $p \to 0$ can be also approximated with Poisson distribution), set by the following formula: $P_n(m) = c_n^m \times p^m (1-p)^{n-m}$ where $c_n^m = \frac{n!}{m!(n-m)!}$. Final values were corrected taking into account the cumulative probability. Statistics were performed with Statistica (StatSoft.).

# Results

Neurons were selectively stained by injection of the membrane-impermeable $Ca^{2+}$ indicators Fura-2 or Calcium Green-1 dextran into axons of l-ACT PNs for dendrite recordings in the AL, and axon bundles of cKCs for recordings in the MB lip or clusters of somata for PN bouton recordings in the MB lip (Figure 1.1A). Both dyes have similar $Ca^{2+}$ binding affinities and kinetics and therefore resolve the intracellular $Ca^{2+}$ dynamics equally well (Konishi and Watanabe, 1995; Kreitzer et al., 2000).

### Response properties of l-ACT PN dendrites (AL glomeruli)

Dendritic $Ca^{2+}$ signals of PNs were recorded in the AL glomeruli (Figure 1.2A). Previous studies have shown that glomerular $Ca^{2+}$ transients correlate with the action potential activity of PNs which arborize in the same glomerulus (Galizia and Kimmerle, 2004). Therefore we considered the glomerular $Ca^{2+}$ signal of PN dendrites as a monitor for the activity of individual PNs at the output side of the glomerulus.

We measured signals from l-ACT PNs. These neurons are uniglomerular, and receive afferent input from one of about 70 glomeruli on the dorso-rostral part of the AL (Flanagan and Mercer, 1989; Galizia et al., 1999a). On the average 27 ± 0.5 (mean ± SEM) of these 70 glomeruli were visible in each animal (Figure 1.2A). 370 glomeruli from 14 bees were imaged. As previously shown (Sachse and Galizia, 2002), PNs showed background activities in the absence of olfactory stimulation. Odor pulses evoked combinatorial activity patterns in PN dendrites across glomeruli (Figure 1.2B). Intracellular calcium also increased in their somata. Most of the dendritic PN responses were excitatory (98.5 %), but some (1.5 %) were inhibitory. Signal size ranged from 0.5 to 8 % (2.41 ± 0.02 %, $\Delta F/F$, mean ± SEM). Responses were phasic-tonic and/or complex, which corresponds to the temporal dynamics observed for intracellularly recorded spike rates (Abel et al., 2001; Müller et al., 2002; Galizia and Kimmerle, 2004) (Figure 1.2C). Of the 27 glomeruli accessible from the frontal aspect, 5.3 ± 0.7 (mean ± SEM) were activated by any of the 4 odors presented, resulting in a glomerular response probability of $p_G = 0.20 \pm 0.02$ (mean ± SEM) per PN and odor.

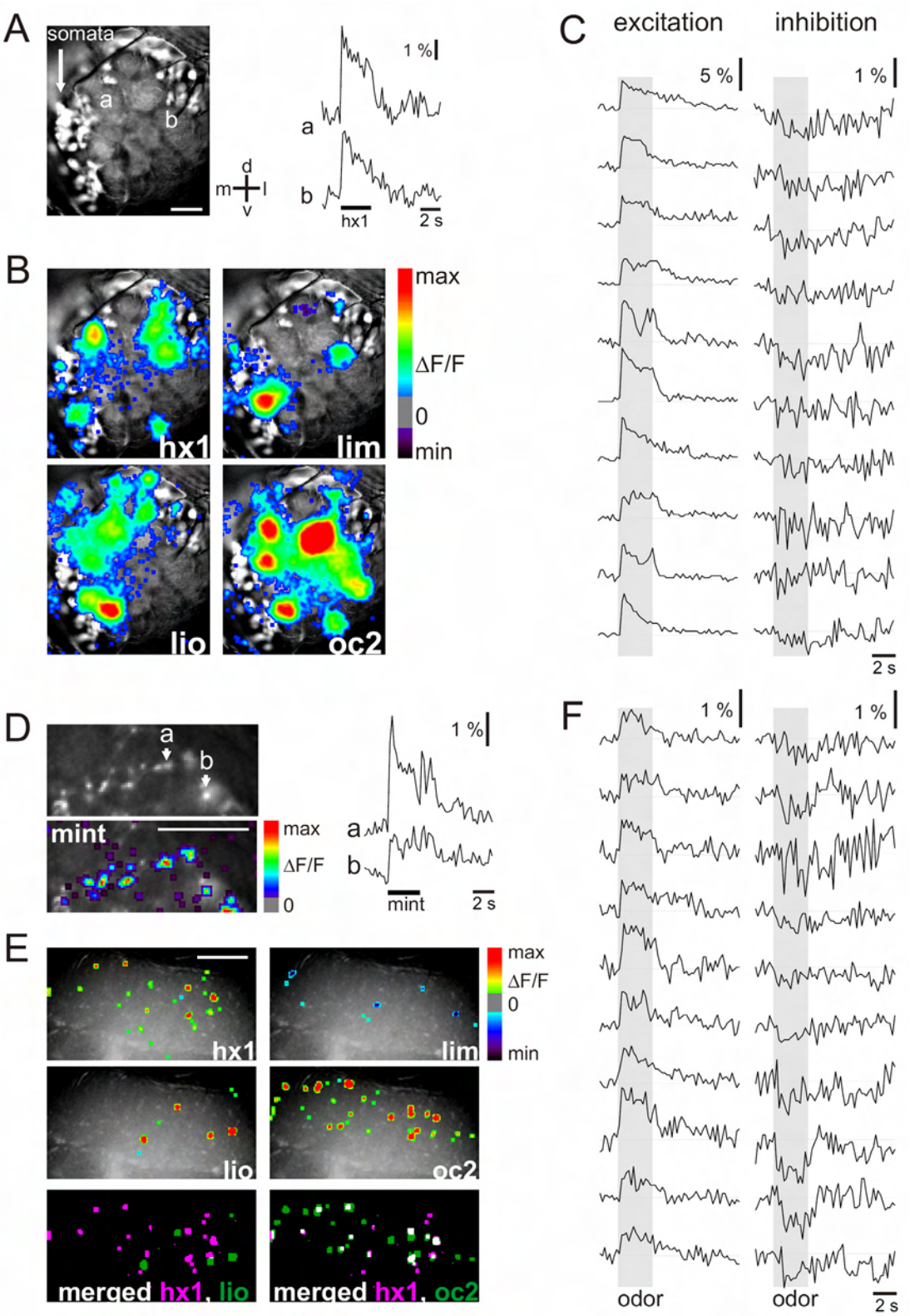
A
somata
a
b
d
m
l
v
1 %
a
b
hx1
2 s
B
max
ΔF/F
0
min
hx1
lim
lio
oc2
C
excitation
inhibition
5 %
1 %
2 s
D
a
b
mint
max
ΔF/F
0
1 %
a
b
mint
2 s
E
hx1
lim
lio
oc2
max
ΔF/F
0
min
merged hx1, lio
merged hx1, oc2
F
1 %
1 %
odor
odor
2 s

**Figure 1.2**

**Figure 1.2 Response properties of l-ACT projection neurons**

**(A)** Dendritic responses to odor stimulation in uniglomerular l-ACT PNs imaged in the frontal AL glomeruli. Traces represent the time courses of Ca2+ transients evoked by 1-hexanol in two glomeruli (a, b). d: dorsal, m: medial, l: lateral, v: ventral **(B)** Color coded Ca2+ signals superimposed on the raw fluorescence image show that different odors activated overlapping combinatorial sets of PN dendrites. **(C)** Traces show representative excitatory and inhibitory dendritic odor responses in the AL (N= 10 bees). Ca2+ transients typically followed complex temporal dynamics. Odor stimulus is highlighted. **(D)** Odor responses in axon terminals (boutons) of PNs in the MB calyx. Boutons are visible in the raw fluorescence image. Stimulation with peppermint induced Ca2+ increase in many of the boutons (single measurement). **(E)** Different odors evoked excitatory and inhibitory responses in distinct boutons. The merged images of excitatory 1-hexanol (hx1, red) and linalool (lio, green) responses visualize distinct sets of activated boutons. In contrast, 1-hexanol (red) and 2-octanol (oc2, green) activated overlapping sets of boutons. All traces represent single measurements; images represent the averages of 3 stimulations. **(F)** Odor-evoked Ca2+ transients in PN boutons (N= 8 bees) show complex dynamics as is the case in the dendrites. In the entire Figure, traces ΔF/F; scale bars 50 µm

## Response properties of l-ACT PN boutons (MB calyx)

To investigate the relationship between AL output and MB input carried by PNs, we next examined the response properties of PN boutons in the MB calyx. PN boutons were selectively filled with the $Ca^{2+}$ indicator via l-ACT soma clusters located on the dorso-medial surface of the AL (Figure 1.2A). We recorded from a total of 105 responsive boutons (9 bees) in the frontal lip area of the median calyx. Odor-induced responses consisted of isolated activity spots, which were colocalized with boutons visible in the raw fluorescence image (Figure 1.2D). 87.2% of the responses were excitatory, with fluorescence changes ranging from 0.3 to 3.8 % (0.87 ± 0.03 % ΔF/F, mean ± SEM), whereas the remaining 12.8 % of the responses were inhibitory. As is the case in the AL, stimulation with odors activated odor-specific ensembles of PN boutons (Figure 1.2E). Boutons were located at different focal depths, and were not always visible in the raw fluorescence image, so that we did not determine their response probability. In the absence of odor stimulation baseline fluorescence showed strong fluctuations, similar to the background activity found in the dendrites of these cells, in the AL glomeruli (see above). These fluctuations were not further analyzed because the signal to noise ratio was rather low.

The response dynamics of PN boutons resembled those of PN dendrites (glomeruli). They showed phasic-tonic and/or complex time courses and often outlasted the odor pulse by several seconds (Figure 1.2F). The across-odor response profile of the PN boutons also resembled the one observed in PN dendrites (Figure 1.3): Limonene odor elicited fewer responses than the other 3 tested odors, and glomeruli and boutons responding to 2-octanol often also responded to 1-hexanol. However, in boutons the proportion of inhibitory responses was higher than in glomeruli (12.8 % vs. 1.5 %).

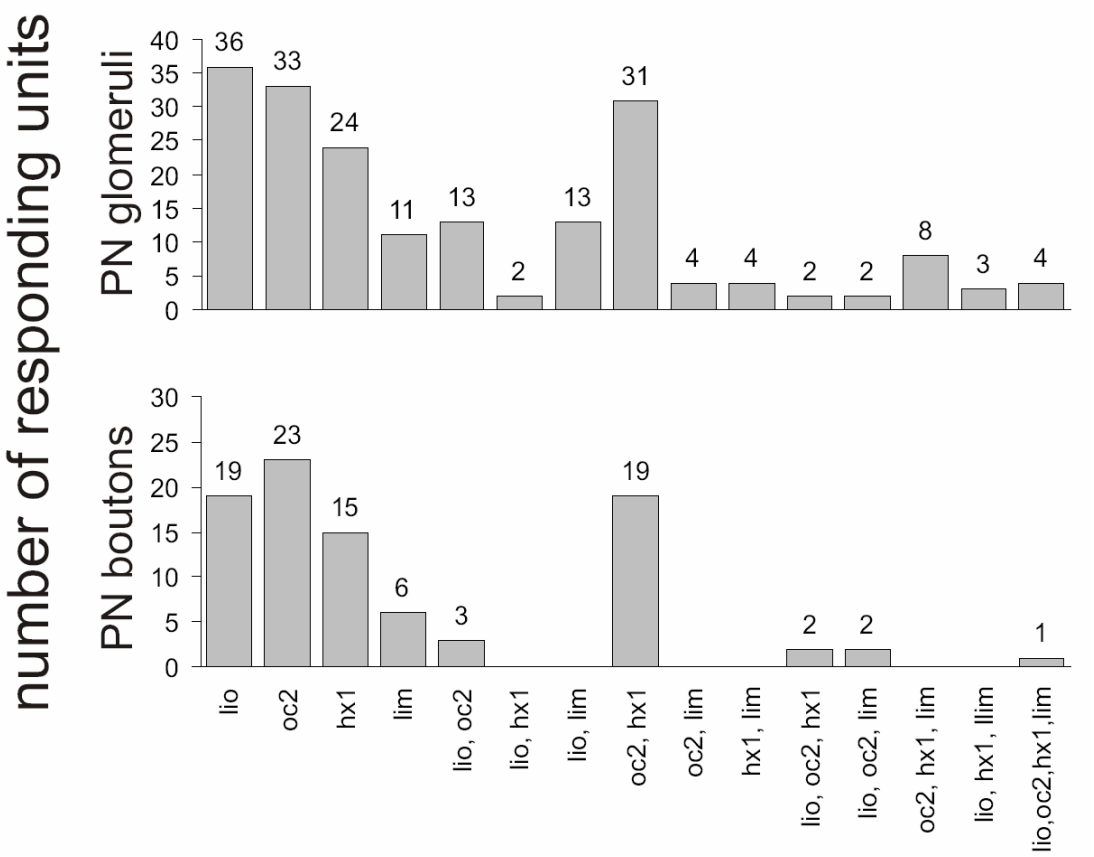


**Figure 1.3 Response profiles of l-ACT projection neuron dendrites and boutons**

Histograms show the number of PN glomeruli (measured as PN dendrites) and PN boutons (measured in the calyces) which responded to either one or more odors. Both PN dendrites and boutons showed fewer responses to limonene than to the other three odors. 2-octanol and 1-hexanol activated overlapping sets of glomeruli and boutons, respectively. Boutons showed fewer overlapping responses than dendrites. (PN dendrites measured in 190 glomeruli in N = 11 bees, 90 boutons in N = 8 bees).

**Response properties of cKC (MB calyx)**

In the MB calyx, l-ACT PNs synapse onto cKC, a population of cells intrinsic to the MBs. In order to investigate how odor information is processed within the MB, we therefore recorded from cKCs. cKCs can be reliably identified based on their anatomy (Figure 1.4A, B). They differ from other KC types in that they feature a columnar arrangement of their unbranched dendrites, which possess 5 to 10 claw-like synaptic structures. Their somata (3 to 7 µm in diameter) are located outside the calyx region rostral to the lip and are connected to the dendrites through a 10 to 100 µm long primary neurite. Dendrites and somata of these cells were selectively stained by injecting Fura-2 dextran into their axons in the ventral part of the α-lobe. Dendritic and somatic responses to odors were then recorded in the lip region of the MB calyx. Figure 1.4B shows an example where only one cKC was stained. Its soma and dendritic branches were visible in the fluorescence image. The time courses of $Ca^{2+}$ transients in dendrite and soma were similar. Both followed a uniform phasic upraise at stimulus onset with off-responses after the end of the odor stimulus. However, $Ca^{2+}$ signal decay was slower in the somata.

In the soma layer odors induced sharp activity peaks in individual cKC somata, which showed fluorescence changes ranging from 0.3 to 2.7 % (1.09 ± 0.03 ΔF/F, mean ± SEM, 67 responses in 8 bees). In the lip neuropil of the calyx, odor-induced dendritic activity appeared in larger, less well-defined regions and showed fluorescence changes ranging from 0.5 to 6 % (1.49 ± 0.03% ΔF/F, mean ± SEM, 473 responses in 15 bees). Those activity patches had a columnar or elongated shape of 20 to 60 µm in diameter, which matches the morphology of the dendritic trees of single cKCs (Figure 1.4B, D). Dendritic activity patches and activated somata often occurred close to each other, indicating that they belong to the same cKC. Response dynamics were common among cKCs. Figure 1.4C shows 10 representative dendritic cKC responses. cKC exclusively exhibited excitatory responses. Off-responses were visible in 40 % of the measurements.

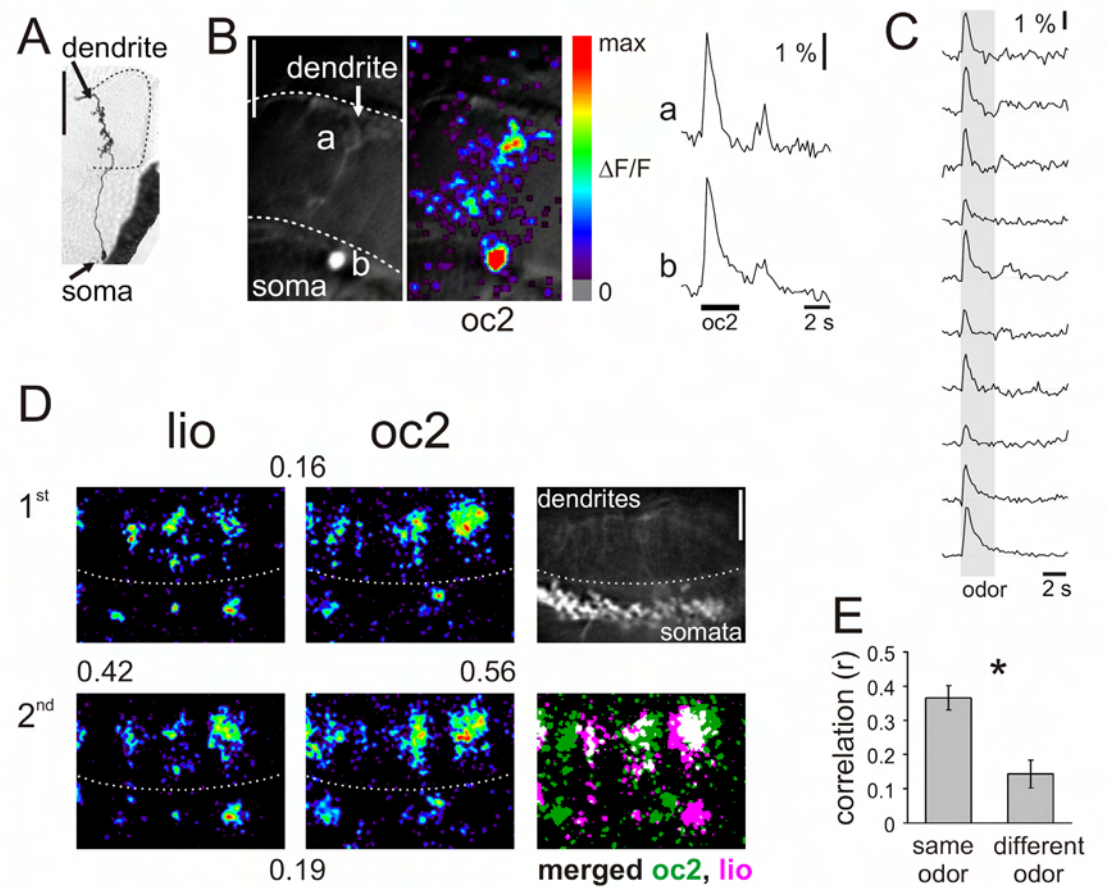


**Figure 1.4 Response properties of clawed Kenyon cells**

**(A)** Golgi stain (adapted from Rybak and Menzel, 1993; with permission) of a cKC in the MB calyx lip region (outlined with dashed lines). **(B)** Fura-fluorescence of a single cKC in the calyx lip. The soma and dendrite are visible in the fluorescence image. Stimulation with 2-octanol (oc2) evoked Ca2+ transients in both the dendrite (a) and soma (b). The Ca2+ dynamics were similar in the soma and dendrite. They followed a characteristic phasic time course and exhibited off-responses after the end of the stimulus. However, in the somata the decay of the Ca2+ transient was slightly slower than in dendrites. **(C)** Time courses of representative dendritic odor responses. Ca2+ dynamics were uniform across animals (N= 10 bees). **(D)** Mass staining of cKCs and Ca2+ signals evoked by 2-octanol (oc2) and linalool (lio). The two odors activated different combinatorial activity patterns of cKC somata and dendrites with some regional overlap. Numbers represent the correlation (r) between the images. **(E)** The correlation between response patterns which were elicited by repeated presentations of the same odors was always higher than between response patterns to different odors (n = 15 bees, 2 two 4 odors per bee, linear correlation, Wilcoxon Signed Rank Test, $p < 0.001$). Scale bars 50 µm; traces ΔF/F

Different odors induced different patterns of activated cKC dendrites with different degrees of overlap, while stimulation with the same odor reliably activated the same cKC ensembles (Figure 1.4D). To confirm the odor specificity of the spatial response patterns, the correlation coefficient between dendritic activity patterns was calculated as a measure of similarity. The correlation coefficients were generally low, which can be attributed to the fact that only a small surface of the imaged area was activated by any one stimulus, so that correlation coefficients were strongly influenced by the noise in the non-responding areas. The mean correlation coefficient between responses which have been elicited by repeated presentation of the same odor was always higher than between responses to different odors (0.37 ±0.04 vs. 0.14 ± 0.04, Wilcoxon Signed Rank Test, $p<0.001$, $n = 15$) (Figure 1.4E).

Due to the limited spatial resolution of the signal it was not possible to determine whether the overlap between the dendritic activity patches reflects responses from the same cKC or from cKCs with anatomically overlapping dendritic trees. However, we found that the responses in somata mirrored the activity of their corresponding dendrites. Therefore we quantified the response properties of individual cKCs by analyzing the activity of somata as a monitor for individual KCs. We recorded from 1680 cKC somata in 12 animals, which were exposed to all four odors. 77 somata responded to at least one of the four tested odors. Odors activated non-overlapping cKC ensembles. The response probability of a given cKC was $p_{KC} = 0.013 \pm 0.001$ (mean ± SEM) per odor.

**Sparsening of the population code in the MB**

In order to analyze the transformation of odor representations in the MB and to evaluate the contribution of pre- and postsynaptic processing, we compared the responses of PN dendrites, PN boutons and cKCs to the four tested odors (1-hexanol, 2-octanol, limonene and linalool). We first asked whether odor processing along the olfactory pathway leads to a change in the sparseness of the population code. The population sparseness of a neural code is a measure for the degree of overlap between neural representations of sensory stimuli (Willmore and Tolhurst, 2001; Olshausen and Field, 2004). A sparse neural code is characterized by a small proportion of active neurons at any time (population sparseness) and/or by a narrow tuning width of

responsive units (lifetime sparseness), resulting in a low degree of overlap between odor-coding ensembles.

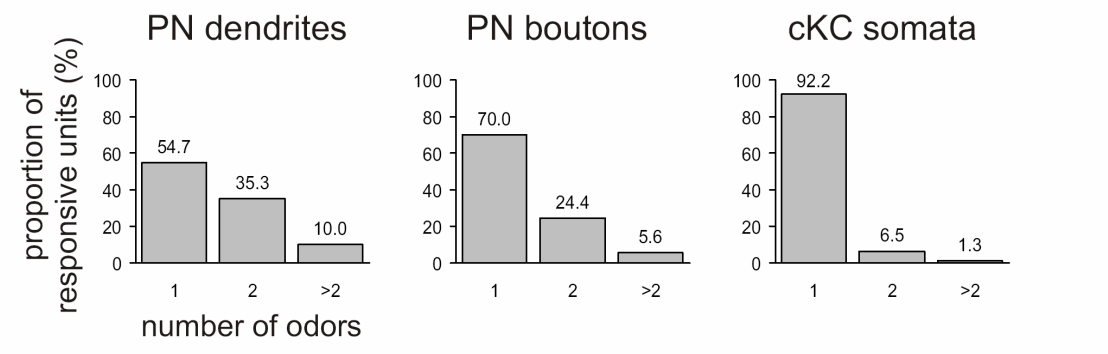


**Figure 1.5 Progressive sparsening of population responses in the MB**

The histograms show the percentage of responsive units (PN dendrites measured in the glomeruli, PN boutons, and cKC somata) which were activated by 1, 2, or more odors (4 odors were presented). The distributions varied significantly between the different processing stages and showed a progressive increase in the sparseness of odor representations from PN dendrites to PN boutons and to cKCs (Chi-square test, applied on absolute numbers of responsive units, $p<0.001$; PN dendrites: n = 298 responsive glomeruli in 14 bees; PN boutons: 90 responsive in 9 bees; cKCs: 77 responsive somata in 12 bees).

Figure 1.5 illustrates the progressive sparsening of the odor code from PN dendrites to PN boutons and to cKC somata. In the AL, PNs were broadly tuned since many glomeruli respond to more than one odor. PN boutons were more narrowly tuned, as the histogram was skewed towards a lower number of odors. cKCs showed the highest sparseness, were extremely odor specific and most responded to one odor only. This result demonstrates that odor processing in the MB results in a sparsening of the odor code carried by cKCs. Furthermore it indicates that sparsening of the population code occurs not only at the level of the postsynaptic cKCs, but, to a lower extent, also at the presynaptic terminals of the PNs. Thus the high degree of sparseness at the KC level can be attributed to at least two distinct processes.

### Change in response dynamics

Understanding the logic of sensory information coding requires the identification of those features of the neural representations which are read out by downstream neurons. We therefore tried to narrow down features of the PN responses which might be read out by cKCs. Odor-evoked activity patterns of PNs are not stationary, but show temporal modulations, which evolve over time and lead to activity patterns that in several species are most odor-specific after some hundreds of milliseconds

following odor onset (bee: Galizia et al., 2000; Galán et al., 2004; locust: Stopfer et al., 2003; zebrafish olfactory bulb: Friedrich and Laurent, 2001). It has been suggested that downstream neurons have to read out these temporal patterns to retrieve the odor information. If that is true, then the temporal patterns of PN responses must be relevant for KCs, and KCs tuned to PN activity patterns should respond with time lags corresponding to particular phases of the dynamic response.

To test this hypothesis we investigated the temporal relationship between PN and cKC responses by simultaneously recording from PN boutons and cKC using two different dyes. The traces in Figure 1.6A show $Ca^{2+}$ transients measured at 5 Hz in individual PN boutons and colocalized KC dendrites. There was no detectable time lag between the responses of PN boutons and cKCs, indicating that the delay of transmission was well below the 200 ms cycle duration in the recordings. In order to get a more accurate estimation of the delay between PN boutons and KC responses we compared response onsets to 3 s odor pulses. Only animals with signal/noise ratios above 5 were chosen, and three measurements were averaged (PNs: 3 times 655 measurements in 11 bees; KCs: 3 times 184 measurements in 15 bees).

Most of the PNs responded with constant delays. 90 % of the responses occurred within 400 ms after stimulus onset, while the remaining 10% showed delays of up to 1000 ms. 95 % of the KC responses occurred within 400 ms after stimulus onset and the remaining 5 % occurred within 400 to 600 ms. No KC responded at a later time point. Figure 1.6B shows the time courses of $Ca^{2+}$ signals in PN dendrites, boutons and KCs, and illustrates the relationship between the response dynamics of PNs and KCs. Even though PN activity was temporally complex during an odor stimulus of 3 sec and often outlasted the odor stimulus, responses in KCs were always limited to brief phasic responses. Clawed KC responses, therefore, were not influenced by the temporal pattern of PN activity that developed over several hundred ms. These results show that KCs respond to less than the first 200 of ms of the PN response, while later input does not lead to KC activity. The results also demonstrate that the temporal sharpening of the KC response reflects postsynaptic processing, since it is not present in PN boutons.

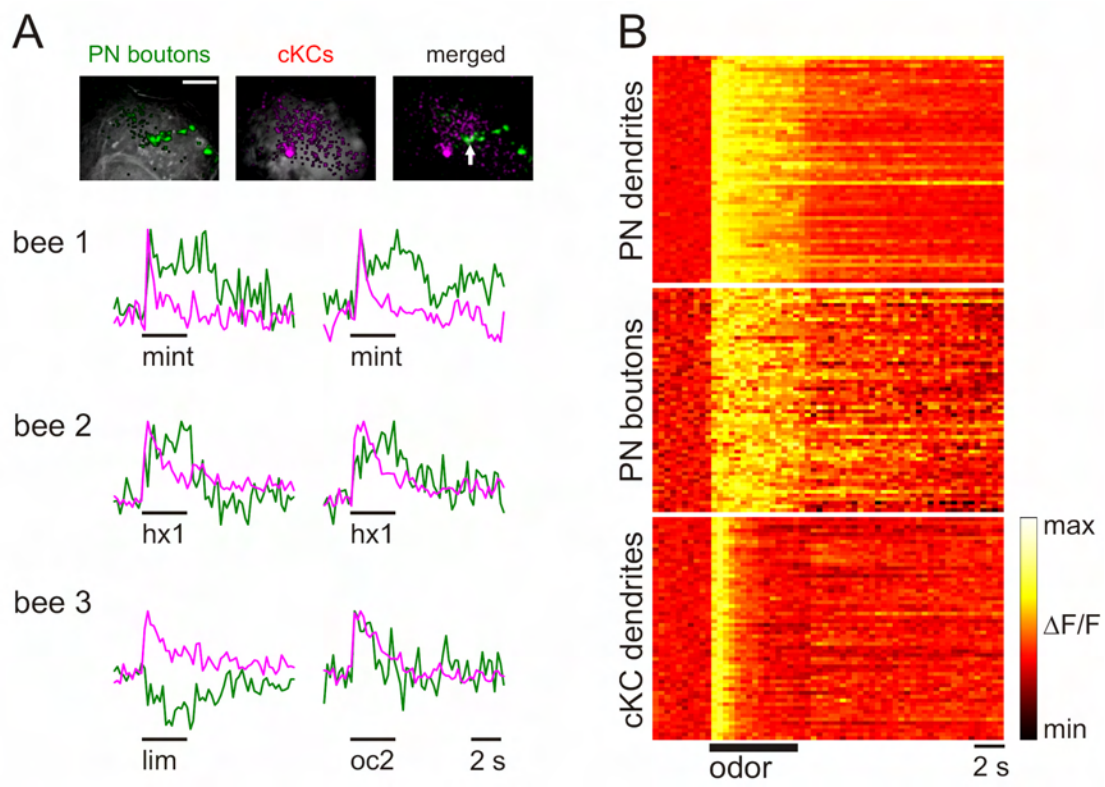


**Figure 1.6 Sharpening of response dynamics in the MB**

(A) l-ACT PN boutons and clawed KCs were stained with different Ca2+ indicators (PNs: Calcium Green-1, KCs: Fura-2) and their odor responses were simultaneously recorded in the MB calyx lip. The merged images display overlapping PN bouton and cKC activities. The traces represent responses in a PN bouton and in cKC dendrites located in the same area (arrow) and for two further bees. The Ca2+ transient of the PN bouton responses typically followed a tonic time course, while the cKC dendrites showed a phasic dynamic. No time lag was observed between PN and cKC bouton responses. Note the off-response of the dendritic KC signal coinciding with the end of the PN responses in bee 2. (B) In each block the time courses of 60 individual glomeruli (PN dendrites), PN boutons or KC dendrites are depicted, each recorded for 12 sec. The odor stimulus is marked with the black bar. The signal intensity is color-coded. cKCs transformed the long-lasting and complex PN input into brief responses. Traces were normalized to the maximum of the absolute signal amplitude. Images and traces represent single measurements. Scale bar 50 µm; traces ΔF/F normalized to maximum

Figure 1.7 elucidates our findings and illustrates a proposed mechanism that may mediate the transformation of odor representations along the olfactory path (see discussion): Within the AL odors evoke dense across-fiber patterns of l-ACT PNs. The spatial activity pattern of the presynaptic terminals of these projection neurons is sparsened within the MB lip - presumably through reciprocal microcircuits between GABAergic neurons and l-ACT PNs. cKCs integrate l-ACT PN activity within 200 ms and transform the complex temporal pattern into brief phasic responses. The sharpening of cKCs' temporal responses may be mediated by a more global inhibition via GABAergic feedback neurons. Moreover the PN-to-KC divergence together with a high spiking threshold may lead to a further sparsening of cKC population responses.

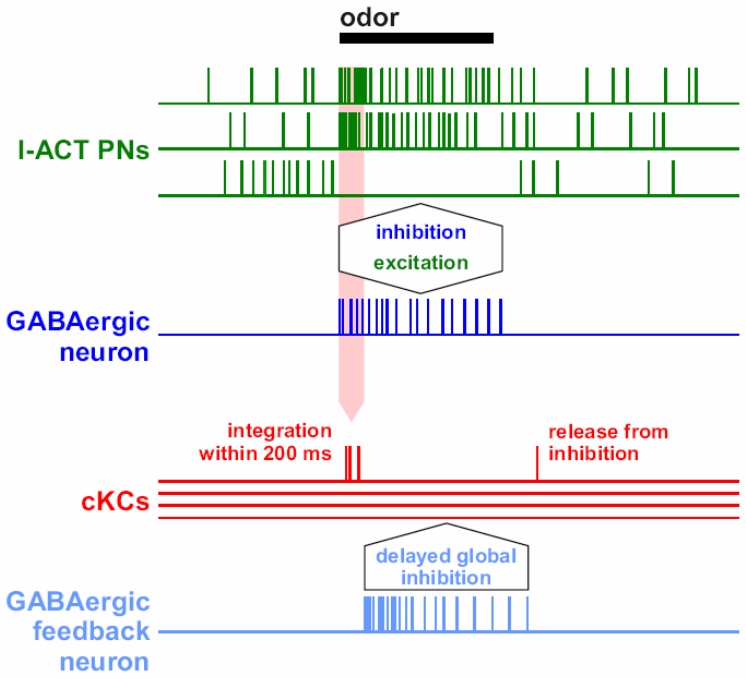


**Figure 1.7 Model of odor processing in the MB input**

l-ACT PNs (green) convey odor information in form of dense across-fiber patterns of action potential bursts. In the MB input they make excitatory synapses with cKCs (red) and with terminals of extrinsic GABAergic neurons (dark blue), which, in turn, make inhibitory synapses with PN boutons. The inhibitory input onto PN boutons has the effect that not all boutons of an excited PN will respond, resulting in a sharpening of the response profiles of PN boutons. GABAergic feedback neurons (light blue), which receive input from a large number of KCs (presumably excluding cKCs), form a global inhibitory loop and mediate delayed, odor-driven inhibition of cKCs. The inhibitory input onto cKCs restricts their integration time window for PN input to less than 200 ms, and shortens their response duration. After the end of the odor stimulus the inhibitory input declines and cKCs are released from inhibition and become excitable again. Since many PNs continue spiking after the end of the odor stimulus some cKCs exhibit off-responses. The divergent connectivity between l-ACT PNs and cKCs, together with a high spiking threshold of cKCs, leads to a further sparsening of cKCs' population response.

# Discussion

We characterized the transmission of odor-evoked activities along three consecutive processing stages and analyzed pre- and postsynaptic mechanisms that underlay odor processing in the insect MBs. We found that odor coding in the AL and the MBs are fundamentally different. The representation of odors in the MBs is sparse across the population of cKC, and this sparsening occurs in two separate steps, one presynaptic and the other postsynaptic at the PN-KC synapse. Furthermore, odor representation in cKCs is temporally sparse, indicating that at most the initial 200 ms of an odor response are relevant for cKC responses. This has profound implications for how information can be used for olfactory recognition and memory formation.

### Methodological aspects and signal source

To investigate the spatial and temporal properties of odor processing in the MB, we measured $Ca^{2+}$ transients in l-ACT PN dendrites in the AL, in their presynaptic axon terminals in the MB, and in their postsynaptic partners, the cKCs. Do the $Ca^{2+}$ signals recorded in these different neural sub-structures allow the comparison between spatio-temporal activity patterns? The signals would be comparable if the mechanisms for generating the measured $Ca^{2+}$ transients did not differ qualitatively.

We hypothesize that the measured $Ca^{2+}$ transients in the three sub-structures are all dominated by calcium influx through voltage-activated calcium channels, and therefore qualitatively reflect the electrical activity of their respective cell compartment, as would be measured electrophysiologically. For PN dendrites, intracellular recordings and subsequent $Ca^{2+}$ imaging of the corresponding glomerulus have shown that $Ca^{2+}$ transients are directly related to their action potential rates, i.e. PNs which responded to an odor with increased spiking also responded with an increase in dendritic $Ca^{2+}$ (Galizia and Kimmerle, 2004). Studies in many neurons from a variety of species showed that pre- and postsynaptic $Ca^{2+}$ transients measured with Fura-2 or Calcium Green-1 are dominated by $Ca^{2+}$ influx through voltage-gated channels which open due to action potential (Svoboda et al., 1997; Oertner et al., 1999; Charpak et al., 2001; Kurtz et al., 2001; Single and Borst, 2002; Wachman et al., 2004). Electrophysiological recordings in the locust have shown that KCs have a low baseline activity of 0.025 spikes per s (Perez-Orive et al., 2002). This is in

agreement with the low level of cKCs' $Ca^{2+}$ fluctuations in the absence of odor stimuli found in our experiments. A low intracellular $Ca^{2+}$ level would also explain why cKCs exclusively exhibited excitatory responses, even though they presumably receive odor-driven inhibition (see below), since the low $Ca^{2+}$ level would not be further decreased by inhibitory input.

We confined the area monitored in the MB to the frontal part of the lip for technical reasons. We assume that the properties of PN boutons and cKCs located in this area are representative for any other part of the MB lip. Within the MB calyx, KCs of different types and sensory modalities are arranged in concentric layers. Olfactory KCs are homogenously distributed along the lip layer, where they receive input from the l-ACT PN boutons (Mobbs, 1982). Although l-ACT PN boutons are not homogenously distributed (Müller et al., 2002), the recorded area was large enough to contain several boutons of each PN.

Besides l-ACT PNs recorded in this study, m-ACT PNs also project onto the lip area. m-ACT PNs receive input from an area in the AL that was not accessible for our imaging technique. Müller et al. (2002) found that m-ACT and l-ACT PNs differ in their response properties. Unlike l-ACT PNs, m-ACT PNs show odor-specific response latencies of several 100 ms. Since cKCs exhibit stable and immediate responses, we conclude that the recorded responses of cKCs are exclusively driven by l-ACT PNs. In the same area where we recorded from cKCs, there are other KCs (Type 1 KCs) that might be the preferential targets for m-ACT PNs. It is likely that such KCs receiving input from m-ACT PNs have very different response properties from the cKCs described here, but these KCs were not filled with dye and did not contribute to the recorded signal.

**Transformation of odor coding within l-ACT PNs: dendrites to boutons**

Within the MB lip, PN boutons convey excitatory input to KCs and GABAergic neurons, which in turn provide inhibitory feedback onto the PN boutons themselves (Figure 1.1B) (Ganeshina and Menzel, 2001). To asses the role of these microcircuits for odor processing, we compared the odor responses in PN dendrites within the AL glomeruli with those at the PN boutons in the MBs (Figure 1.2, 1.3). Both PN dendrites and boutons exhibited reliable combinatorial patterns of odor-evoked activity and showed similar response profiles. However, PN dendrites responded less

frequently with inhibition than their boutons (1.5% vs. 12.8%) and were more broadly tuned to odors. We propose that this effect is caused by local inhibition of the presynaptic boutons within the MB lip. The high odor specificity observed in KCs may therefore be generated, in part, by presynaptic inhibition of PN boutons via local recurrent microcircuits.

**Transformation from l-ACT PNs to cKCs: population sparsening**

We have analyzed the response characteristics of l-ACT PNs and cKCs across their population. In both, odors are coded in form of combinatorial activity patterns. However, cKCs with the same olfactory profile are not grouped into functional subunits as is the case for the PNs in the AL, where they all coalesce in one glomerulus. In the absence of consistent landmarks as reference points, we could not assess whether there is a stereotypic organization of responding KCs between individuals, as in *Drosophila* (Wang et al., 2004).

We demonstrated that odor-activated cKC ensembles are sparse compared to PN ensembles. Unlike PNs, cKCs responded very selectively to odors. The observed response probability $p_{KC}$ of a given cKC averages 0.013 per odor and is significantly lower than the response probability of PN dendrites ($p_G$ = 0.2). The observed sparseness of the recorded cKCs is in accordance with the finding of a sparse code in KCs of locusts and *Drosophila* (Perez-Orive et al., 2002; Wang et al., 2004) and may therefore represent a general property of KCs. Both the distributive character and the sparseness of the cKC code may be a result of the divergent-convergent connectivity between PNs and cKCs (Laurent, 2002). About 500 l-ACT PNs converge onto estimated 20.000 cKCs (counted and interpolated from Golgi stains, J. Rybak, personal communication). Knowing that each l-ACT PN has approximately 400 boutons (Müller et al., 2002) this yields a ratio of ~10 boutons per cKC. This matches the number of claw-like dendritic specializations in each cKC. Assuming that each of these claws contacts a different PN, how many of these PN inputs must be coactive to induce a cKC response? With a response probability $p_G$ = 0.2 in PNs, a cumulative probability corresponding to cKC activity of $p_{KC}$ = 0.013 is reached when 5.8 or more out of 10 PNs are simultaneously active. Thus, a single cKC would compress information carried by a subset of 6 to 10 PNs. This means that cKCs must have a high firing threshold, which could be the result of the intrinsic properties of KCs

and/or of odor-driven inhibition (Laurent and Naraghi, 1994; Perez-Orive et al., 2002).

**Transformation from l-ACT PNs to cKCs: temporal sharpening**

cKCs had a phasic response with a fast onset of less than 200 ms. This indicates that they decode afferent PN activities only at the beginning of each response bout. This observation conflicts with studies in locusts. There, odors evoke transient spike synchronizations between PNs which develop over hundreds of ms after stimulus onset (Laurent and Davidowitz, 1994; Laurent et al., 1996; Wehr and Laurent, 1996; Stopfer et al., 2003) and lead to KCs which respond with variable, odor-specific latencies (Perez-Orive et al., 2002; Stopfer et al., 2003). The short and stable time-lag between responses in l-ACT PNs and clawed KCs in the bee excludes the possibility that odor information might be decoded from spike synchrony events which evolve over hundreds of ms. However, it does not rule out the possibility that coincident PN spikes are a necessary component of the olfactory code during the initial 200 ms of an odor response.

What are the mechanisms underlying the short integration time and the sharp response dynamics of cKCs? We assume that both result from odor-driven delayed inhibition of cKCs. Odor-driven inhibitory input was found in locust KCs (Laurent and Naraghi, 1994; Perez-Orive et al., 2002). The response dynamics of bees` cKCs provide clear evidence that they might receive inhibitory input as well. Despite continuous input from PNs, cKCs' response onset was restricted to the beginning of PNs' response, and followed a phasic time course (Figure 1.6B). There were no cKCs which responded at a later time point. This indicates that cKCs might indeed receive delayed odor-driven inhibition which lasts as long as the odor stimulus and prevents them from spiking again. Candidate neurons for the presumed odor-driven delayed inhibition of KCs are GABAergic feedback neurons, which receive input from a large population of KCs in the MB pedunculus and lobes, presumably leaving out the cKCs, and project back to the lip of the MB (Schäfer and Bicker, 1986; Grünewald, 1999a). The response properties of those feedback neurons correspond with their putative function of mediating inhibition of cKC dendrites which arrives with a delay relative to the excitatory PN input (Grünewald, 1999b). They exhibit phasic-tonic odor responses which usually do not exceed stimulus duration. Thus, the off-responses of cKCs after

the stimulus offset could reflect release from inhibition that makes them once again sensitive for input from PNs which remain active after stimulus offset.

The finding that cKCs integrate PN output within a time window below 200 ms does not necessarily imply that PN action potentials arriving later are irrelevant for odor processing. First, PNs also have output synapses within the AL, and their later activity may be relevant to processes within the AL (Sachse and Galizia, 2005). Second, late PN responses could be read out by other target neurons outside the MBs, such as the neurons in the lateral horn. Third, class I KCs, from which we did not record but which also arborize in the lip region of the MB calyx, may be sensitive for late PN activities and may have different response properties. It is tempting to speculate more about the possible differences between class I KCs and cKCs. They might constitute two parallel pathways of olfactory information processing in the MB. Class I KCs are likely to read out input from m-ACT PNs, since these neurons innervate the same lip area, but are not read out by the cKCs (see above). m-ACTs exhibit a more complex temporal response pattern, including odor-specific response delays and low-frequency spiking (Müller et al., 2002). If they receive additional direct or indirect input from l-ACT they could relate these activities to the timing of stimulus onset, so that the odor-specific delay of m-ACT input can be detected and decoded. cKCs, in turn, would read out olfactory information that is provided by the fast response onset of a specific combination of l-ACT PNs.

l-ACT PNs and cKCs may play a dominant role in odor learning. Imaging experiments in bees showed that, in the AL, glomeruli innervated by l-ACT PNs show learning-induced modulations of their responses to odors (Faber et al., 1999). Clawed KCs of the γ-lobe in *Drosophila* are particularly important for olfactory short-term memory (Zars et al., 2000). Due to the anatomical similarities between clawed KCs in bees and *Drosophila*, it has been suggested that they are homologues (Strausfeld, 2002). Accordingly, the clawed KCs recorded in our study might play a major role in memory formation. Indeed, the code used by l-ACT PNs and cKCs might be ideally suited for computations underlying odor learning. Each odor is encoded in a quasi-simultaneous combinatorial pattern of active cKCs without complex temporal activity sequences, which is an ideal substrate for associative learning rules of a Hebbian type (Lechner and Byrne, 1998).

## Acknowledgments

This work was supported by grants from the Deutsche Forschungsgemeinschaft. I am grateful to Jürgen Rybak and Ana Florencia Silbering for helpful discussions and Mary Wurm for correcting the manuscript.

# References

Abel, R., Rybak, J., and Menzel, R. (2001). Structure and Response Patterns of Olfactory Interneurons in the Honeybee, *Apis mellifera*. J. Comp. Neurol. *437*, 363-383.

Bicker, G., Kreissl, S., and Hofbauer, A. (1993). Monoclonal antibody labels olfactory and visual pathways in Drosophila and Apis brains. J. Comp. Neurol. *335*, 413-424.

Charpak, S., Mertz, J., Beaurepaire, E., Moreaux, L., and Delaney, K. (2001). Odor-evoked calcium signals in dendrites of rat mitral cells. Proc. Natl. Acad. Sci. USA *98*: 1230-1234.

Davis, R.L. (1993). Mushroom bodies and Drosophila learning. Neuron *11*, 1-14.

Faber, T., Joerges, J., and Menzel, R. (1999). Associative learning modifies neural representations of odors in the insect brain. Nat. Neurosci. *2*, 74-78.

Farris, S.M., Abrams, A.I., and Strausfeld, N.J. (2004). Development and morphology of Class II Kenyon cells in the mushroom bodies of the honey bee, Apis mellifera. J. Comp. Neurol. *474*, 325-339.

Flanagan, D. and Mercer, A.R. (1989). An atlas and 3-D reconstruction of the antennal lobes in the worker honey bee, Apis mellifera L. (Hymenoptera: Apidae). Int. J. Insect Morphol. Embryol. *18*, 145-159.

Friedrich, R.W. and Laurent, G.J. (2001). Dynamic optimization of odor representations by slow temporal patterning of mitral cell activity. Science *291*, 889-894.

Galán, R.F., Sachse, S., Galizia, C.G., and Herz, A.V.M. (2004). Odor-driven attractor dynamics in the antennal lobe allow for simple and rapid olfactory pattern classification. Neural Comput. *16*, 999-1012.

Galizia, C.G., Joerges, J., Küttner, A., Faber, T., and Menzel, R. (1997). A semi-in-vivo preparation for optical recording of the insect brain. J. Neurosci. Methods *76*, 61-69.

Galizia, C.G. and Kimmerle, B. (2004). Physiological and morphological characterization of honeybee olfactory neurons combining electrophysiology, calcium imaging and confocal microscopy. J.Comp. Physiol. A Neuroethol. Sens. Neural Behav. Physiol. *190*, 21-38.

Galizia, C.G., Küttner, A., Joerges, J., and Menzel, R. (2000). Odour representation in honeybee olfactory glomeruli shows slow temporal dynamics: an optical recording study using a voltage-sensitive dye. J.Insect Physiol. *46*, 877-886.

Galizia, C.G., McIlwrath, S.L., and Menzel, R. (1999a). A digital three-dimensional atlas of the honeybee antennal lobe based on optical sections acquired by confocal microscopy. Cell Tissue Res. *295*, 383-394.

Galizia, C.G., Sachse, S., Rappert, A., and Menzel, R. (1999b). The glomerular code for odor representation is species specific in the honeybee Apis mellifera. Nat. Neurosci. *2*, 473-478.

Galizia, C. and Vetter, R. (2004). Optical Methods for Analyzing Odor-evoked Activity in the Insect Brain. In Advances in Insect Sensory Neuroscience, T. Christensen, ed. (Boca Raton, FL: CRC Press).

Ganeshina, O.T. and Menzel,R. (2001). GABA-immunoreactive neurons in the mushroom bodies of the honeybee: An electron microscopic study. J. Comp. Neurol. *437*, 335-349.

Gronenberg, W. (1986). Physiological and anatomical properties of optical input-fibres to the mushroom body in the bee brain. J. Insect Physiol. *32*, 695-704.

Grünewald, B. (1999a). Morphology of feedback neurons in the mushroom body of the honeybee, Apis mellifera. J. Comp. Neurol. *404*, 114-126.

Grünewald, B. (1999b). Physiological properties and response modulations of mushroom body feedback neurons during olfactory learning in the honeybee, Apis mellifera. J. Comp. Physiol. *185*, 565-576.

Heisenberg, M. (2003). Mushroom body memoir: from maps to models. Nat. Rev. Neurosci. *4*, 266-275.

Hildebrand, J.G. and Shepherd,G.M. (1997). Mechanisms of olfactory discrimination: converging evidence for common principles across phyla. Annu. Rev. Neurosci. *20*, 595-631.

Kenyon, F.C. (1896). The brain of the bee - A preliminary contribution to the morphology of the nervous system of the Arthropoda. J. Comp. Neurol. *6*, 134-210.

Konishi, M. and Watanabe, M. (1995). Resting cytoplasmic free Ca2+ concentration in frog skeletal muscle measured with fura-2 conjugated to high molecular weight dextran. J. Gen. Physiol. *106*, 1123-1150.

Kreitzer, A.C., Gee, K.R., Archer, E.A., and Regehr, W.G. (2000). Monitoring presynaptic calcium dynamics in projection fibers by in vivo loading of a novel calcium indicator. Neuron *27*, 25-32.

Kurtz, R., Warzecha, A.K., and Egelhaaf, M. (2001). Transfer of visual motion information via graded synapses operates linearly in the natural activity range. J. Neurosci. *21*, 6957-6966.

Laurent, G. (2002). Olfactory network dynamics and the coding of multidimensional signals. Nat. Rev. Neurosci. *3*, 884-895.

Laurent, G.J. and Davidowitz, H. (1994). Encoding of olfactory information with oscillating neural assemblies. Science *265*, 1872-1875.

Laurent, G.J. and Naraghi, M. (1994). Odorant-induced oscillations in the mushroom bodies of the locust. J. Neurosci. *14*, 2993-3004.

Laurent, G.J., Wehr, M., and Davidowitz, H. (1996). Temporal representations of odors in an olfactory Network. J. Neurosci. *16*, 3837-3847.

Lechner, H.A. and Byrne, J.H. (1998). New perspectives on classical conditioning: a synthesis of Hebbian and non-Hebbian mechanisms. Neuron *20*, 355-358.

Menzel, R. (1999). Memory dynamics in the honeybee. J. Comp. Physiol. *185*, 323-340.

Mobbs, P.G. (1982). The brain of the honeybee Apis mellifera I.The connections and spatial organization of the mushroom bodies. Phil. Trans. R. Soc. Lond. B Biol. Sci. *298*, 309-354.

Mombaerts, P., Wang, F., Dulac, C., Chao, S.K., Nemes, A., Mendelsohn, M., Edmondson, J., and Axel, R. (1996). Visualizing an olfactory sensory map. Cell *87*, 675-686.

Müller, D., Abel, R., Brandt, R., Zöckler, M., and Menzel, R. (2002). Differential parallel processing of olfactory information in the honeybee, Apis mellifera L. J Comp. Physiol. *188*, 359-370.

Oertner, T.G., Single, S., and Borst, A. (1999). Separation of voltage- and ligand-gated calcium influx in locust neurons by optical imaging. Neurosci. Lett. *274*, 95-98.

Olshausen, B.A. and Field, D.J. (2004). Sparse coding of sensory inputs. Curr. Opin. Neurobiol. *14*, 481-487.

Perez-Orive, J., Mazor, O., Turner, G.C., Cassenaer, S., Wilson, R.I., and Laurent, G. (2002). Oscillations and sparsening of odor representations in the mushroom body. Science *297*, 359-365.

Rybak, J. and Menzel, R. (1993). Anatomy of the mushroom bodies in the honey bee brain: the neuronal connections of the alpha-lobe. J. Comp. Neurol. *334*, 444-465.

Sachse, S. and Galizia, C. (2005). Topography and Dynamics of the Olfactory System. In Microcircuits: The Interface between Neurons and Global Brain Function. Dahlem Workshop Report 93, (Cambridge, MA: The MIT Press) (in press).

Sachse, S. and Galizia, C.G. (2002). The Role of Inhibition for Temporal and Spatial Odor Representation in Olfactory Output Neurons: A Calcium Imaging Study. J. Neurophysiol. *87*, 1106-1117.

Schäfer, S. and Bicker, G. (1986). Distribution of GABA-like immunoreactivity in the brain of the honeybee. J. Comp. Neurol. *246*, 287-300.

Schröter, U. and Menzel, R. (2003). A New Ascending sensory tract to the calyces of the honeybee mushroom body, the subesophageal-calycal tract. J. Comp. Neurol. *465*, 168-178.

Single, S. and Borst, A. (2002). Different mechanisms of calcium entry within different dendritic compartments. J. Neurophysiol. *87*, 1616-1624.

Stopfer, M., Jayaraman, V., and Laurent, G. (2003). Intensity versus identity coding in an olfactory system. Neuron *39*, 991-1004.

Strausfeld, N.J. (2002). Organization of the honey bee mushroom body: representation of the calyx within the vertical and gamma lobes. J. Comp. Neurol. *450*, 4-33.

Svoboda, K., Denk, W., Kleinfeld, D., and Tank, D.W. (1997). In vivo dendritic calcium dynamics in neocortical pyramidal neurons. Nature *385*, 161-165.

Vosshall, L.B., Wong, A.M., and Axel, R. (2000). An olfactory sensory map in the fly brain. Cell *102*, 147-159.

Wachman, E.S., Poage, R.E., Stiles, J.R., Farkas, D.L., and Meriney, S.D. (2004). Spatial Distribution of Calcium Entry Evoked by Single Action Potentials within the Presynaptic Active Zone. J. Neurosci. *24*, 2877-2885.

Wang, Y., Guo, H.-F., Pologruto, T.A., Hannan, F., Hakker, I., Svoboda, K., and Zhong, Y. (2004). Stereotyped odor-evoked activity in the mushroom body of Drosophila reavealed by green fluorescent protein-based $Ca^{2+}$ imaging. J. Neurosci. *24*, 6507-6514.

Wehr, M. and Laurent, G.J. (1996). Odour encoding by temporal sequences of firing in oscillating neural assemblies. Nature *384*, 162-166.

Willmore, B. and Tolhurst, D.J. (2001). Characterizing the sparseness of neural codes. Network: Comput. Neural. Syst. *12*, 255-270.

Zars, T., Fischer, M., Schulz, R., and Heisenberg, M. (2000). Localization of a short-term memory in *Drosophila*. Science *488*, 672-675.